Marine Biology (2018) 165:45
https://doi.org/10.1007/s00227-018-3300-8

ORIGINAL PAPER

Not-so-simple sieving by ascidians: re-examining particle capture at the mesh and organismal scales

Keats R. Conley[1] · Aviv Ben-Tal[2] · Yuval Jacobi[2,3] · Gitai Yahel[2] · Kelly R. Sutherland[1]

Received: 19 October 2017 / Accepted: 25 January 2018

Abstract

The particle capture mechanisms of biological filters determine the particle spectrum that is ingested by filter-feeding animals. Although ascidian feeding has been extensively investigated, the organismal-scale fluid dynamics and mesh-scale particle-filter interactions are not fully characterized. Fluorescein dye visualization of flow through the branchial sac of the ascidian *Ciona intestinalis* showed organismal-scale flow was laminar and moved both parallel and perpendicular to the mucous mesh. Endoscopic investigations of *Herdmania momus* revealed the mesh-scale filtration process, including the pre-capture velocities, particle approach angles, and mesh behavior. The mesh speed was variable (range 0–0.4 mm s^{-1}). To determine how particle shape affects hydrosol capture, *Styela plicata* was fed differently shaped polystyrene particles (ellipsoids and spheres); sampling the inhaled and exhaled water revealed that microellipsoids (0.3 × 0.7 µm) were captured at significantly lower efficiency (32%) than 1 µm microspheres (86%). The capture efficiency of microellipsoids resembled that of microspheres with a diameter similar to the microellipsoids' minor axis (0.3 µm, 31%) suggesting that the minimum diameter of ellipsoidal particles determines the capture efficiency. Flow near the filter was parallel to the mesh even ~ 10 s of micrometers away, implicating a "crossflow" component to ascidian filtration, where the fluid being filtered is directed along the surface of the filter rather than exclusively perpendicular to it. Collectively, these results suggest that ascidian filtration acts as a hybrid-flow filtration system rather than a classical direct sieve.

Introduction

Filter-feeding particulate food from the surrounding water is a common feeding strategy by organisms spanning a range of sizes, including protists, zooplankton, fish, and whales. Different mechanisms, however, are responsible for bringing particles in contact with the filter-feeding structure (Riisgård and Larsen 2010; Kiørboe 2011). The mechanisms of particle collection can depend on quantitative properties such as particle size (Loudon and Alstad 1990; Sutherland et al. 2010; Conley et al. 2017; Jacobi et al. 2017) and density (Rubenstein and Koehl 1977), qualitative properties such as particle surface properties (Gerritsen and Porter 1982; Dadon-Pilosof et al. 2017; Jacobi et al. 2017) and nutritional quality (Beninger et al. 2007), and also on the hydrodynamics of the filter (Silvester 1983; Labarbera 1984; Silverman et al. 1999). Some common types of filtration include: (1) dead-end sieving (direct flow filtration), (2) crossflow (tangential) filtration, and (3) hydrosol filtration.

The term "sieving" can be used broadly to describe 100% capture of particles larger than the pore size of the filter or appendage (Shimeta and Jumars 1991). However, the term often implicates a set of hydrodynamic criteria, wherein there are only two fluid flows: the feed (raw water that has not yet passed through the filter), which is perpendicular to the filter, and the permeate (water that has passed through the filter) (Fig. 1a). A pressure gradient moves all of the feed

Responsible Editor: S. Shumway.

Reviewed by P. Beninger and E. Ward.

Electronic supplementary material The online version of this article (https://doi.org/10.1007/s00227-018-3300-8) contains supplementary material, which is available to authorized users.

✉ Keats R. Conley
keatsconley@gmail.com

[1] Department of Biology, 5289 University of Oregon, Eugene, OR 97403, USA

[2] The School of Marine Sciences, Ruppin Academic Center, Mikhmoret Campus, 402-970 Mikhmoret, Israel

[3] Department of Zoology, George S. Wise Faculty of Life Sciences, Tel-Aviv University, Tel Aviv, Israel

Published online: 08 February 2018

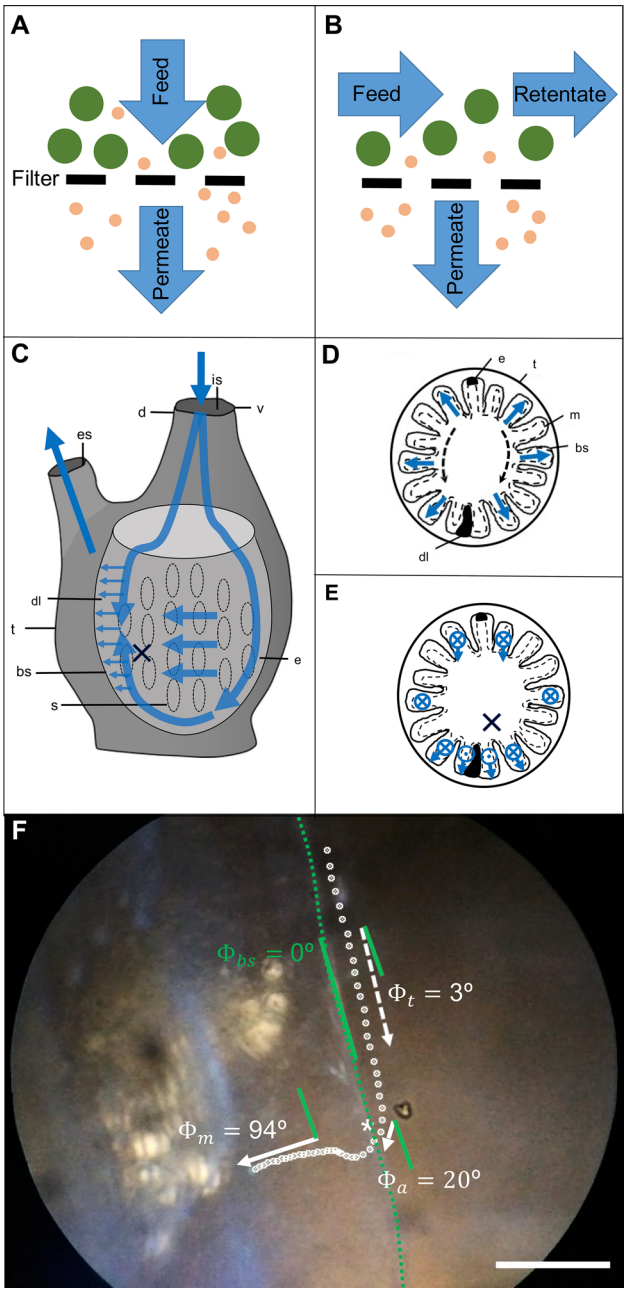

Fig. 1 Schematic of filtration mechanisms and ascidian feeding. **a** ▶ Dead-end sieving. **b** Crossflow filtration. **c** Side view showing water flow through *Herdmania momus*; *is* inhalant siphon, *es* exhalant siphon, *s* stigmata, *t* tunic, *bs* branchial sac, *v* ventral side, *d* dorsal side, *e* endostyle, where mucous mesh is initially secreted, *dl* dorsal lamina, where mucous mesh is collected for ingestion. **d** Cross-section of an ascidian showing classical depiction of water flow through the branchial sac. Branchial sac is shown folded, and black dashed arrows show the direction of mesh movement along the branchial sac; *m* mucous mesh. **e** Cross-section showing proposed depiction of water flow supported by this study. ⊗ indicates flow into the page and ⊙ indicates flow out of the page. **f** Endoscope micrograph showing an anterior–posterior view of the branchial sac of *H. momus*, overlaid with a trajectory of a 4.5 × 13 µm microellipsoid pre- and post-capture (Supplementary video 2). Each point represents one frame. Dashed green line shows the outline of the branchial sac for clarity. The anterior–posterior angle of the branchial sac (Φ_{bs}) was used as the reference (i.e., $\Phi_{bs} = 0°$, solid green line) for measuring the angles of the pre-capture trajectories and particle approach angles, whereas the measurements of ellipsoid orientation (Fig. 7) were made using a different reference, with the flow direction = 0°; Φ_t: angle of trajectory prior to curvature; Φ_a: angle of the microellipsoid as it approaches the mesh; Φ_m: angle of mesh movement. Asterisk indicates position of particle upon contact with the mesh. Black "X" in panel **c** and **e**, shows the approximate position of optical insertion tube in the *y*- and *x*-plane of the branchial sac, respectively. White scale bar 50 µm

through the filter, and particles are captured if they are larger than the filter pores (Li and Li 2015).

In industrial crossflow filtration, there are three flows: the feed, the permeate, and the retentate (concentrated particles) (Bowen and Jenner 1995; Bhave 1997; Mota et al. 2002). As in sieving, the permeate in crossflow filtration is perpendicular to the filter, but the feed and retentate both move parallel to the filter (Fig. 1b) (Bhave 1997). A pressure gradient causes the permeate to diverge orthogonally from the parallel crossflow (Song and Elimelech 1995). As such, crossflow filtration is often used to fractionate large particles from small ones, usually by recirculation of the retentate (Schwartz and Seeley 2002). Industrial crossflow filtration considerably reduces filter clogging due to tangential shearing forces, which lessen the deposition of large particles on the filter surface and delay accumulation of deposited matter (Song and Elimelech 1995; Sanderson et al. 2001). In contrast, large particles in dead-end sieving often accumulate on the filter, reducing its effective pore size and increasing the pressure drop (Schwartz and Seeley 2002). Some biological filters resemble industrial crossflow filters (Brainerd 2001; Sanderson et al. 2001; Smith and Sanderson 2007; Paig-Tran et al. 2013). Video endoscopy of suspension-feeding fishes, for example, revealed that a high velocity crossflow prevented ~ 95% of particles from contacting the filtering gill rakers—an even lower level of particle deposition than is typical of industrial crossflow filters (Sanderson et al. 2001).

Hydrosol filtration predicts capture of particles smaller than the mesh pores via different mechanisms—direct interception, inertial impaction, gravitational deposition, and diffusional deposition—that all cause particles to encounter a filter fiber (Rubenstein and Koehl 1977). The relative influence of the different hydrosol capture mechanisms depends on the Reynolds and Péclet numbers in which the filter operates. Direct interception and diffusional deposition are the primary mechanisms at low Reynolds numbers (Shimeta 1993). Hydrosol filtration can occur independently or may accompany other types of filtration. The particle capture mechanisms of a biological filter determine the particle size spectrum that filter-feeding animals affect and therefore have broad ecological implications (Brainerd 2001; Sanderson et al. 2001).

Ascidians, a class of tunicates, are globally abundant benthic filter-feeders. Solitary ascidians are cylindrically shaped with an inhalant siphon adjacent to an exhalant siphon (Fig. 1c). Throughout the manuscript, we will refer to the orientation of the ascidian using the terminology described by Herdman (1899), where the anterior end refers to the side of the animal where the siphons are located, the posterior end is the region attached to the substrate, the dorsal side is toward the exhalant siphon, and ventral side is away from it (Fig. 1c). Ascidians feed by using cilia to pump water into the inhalant siphon, through the pharynx (branchial sac), and ultimately out the exhalant siphon. The branchial sac is perforated with stigmata, and the beating of the lateral cilia on the stigmata generates the water current (Fig. 1c) (reviewed in Petersen 2007). In some ascidians, the arrangement of the siphons and in situ orientation of the animals also facilitates passive flow by dynamic pressure through the inhalant siphon (Young and Braithwaite 1980; Knott et al. 2004). Turbulence can occur at the inhalent siphon opening, but flow at the filter is viscous and laminar (Kustin et al. 1974; Labarbera 1984). The viscous pump driven by the lateral cilia of the stigmata is considered an energetically undemanding system because of the low pressure drop of the filter (0.1–0.4 mm H_2O) (Jørgensen 1983; Jørgensen et al. 1984; Riisgård 1988).

Particle capture in ascidians occurs by adhesion onto a fine mucous mesh. The dimensions of the ascidian mesh are generally accepted to be ~ 0.5 µm wide × 2 µm long with little variation between species (Flood and Fiala-Medioni 1981; Turon 1990; Petersen 2007), although one study found a finer mesh whose longest dimension did not exceed 0.5 µm (Pennachetti 1984). The mesh is secreted by the endostyle and conveyed dorsally in two separate sheets along the interior surface of the branchial walls by cilia on the secondary structures of the branchial sac (i.e., ciliary mucus transport is separate from the ciliary water current) (Orton 1913; Mackie et al. 1974; Goodbody 1975; Holley 1986). At the dorsal lamina, the mesh is folded into a mucous cord and conveyed to the esophagus for ingestion (Petersen 2007). Textbook descriptions and the primary literature all depict flow in the branchial sac to be exclusively perpendicular to the mucous mesh in all directions (Fig. 1d) (Erika and Werner 1954; Alexander 1981; Jørgensen et al. 1984; Pennachetti 1984; Petersen 2007), except for the endostyle and dorsal lamina, which are non-filtering regions (MacGinitie 1939; Erika and Werner 1954). Particles are prevented from being deposited along the endostyle by an additional set of cilia that effectively redirect particles to the left and right sides of the endostyle (i.e., onto the mucous wall of the pharynx) (Orton 1913; Holley 1986).

Ascidians are considered a characteristic "simple siever" (Riisgard and Larsen 2001; Petersen 2007). They are assumed to feed continuously and non-selectively, with the dimensions of the mucous mesh serving as the primary determinant of the particle size captured (Jørgensen 1966). However, since the ascidian filter uses mucus as an adhesive for captured particles, previous authors have acknowledged that it likely does not function solely by dead-end sieving, but also presumably captures particles via hydrosol filtration (Rubenstein and Koehl 1977; Wotton 1994). The extent to which hydrosol filtration adds to capture of submicrometer particles was recently examined for multiple species of oligotrophic ascidians, which showed relatively high removal efficiency ranging from 31 to 97% for 0.3 µm microspheres (Jacobi et al. 2017). The role of particle shape in determining particle capture has not yet been addressed. In most biological applications of hydrosol filtration theory, particles are assumed to be spherical (Rubenstein and Koehl 1977), which is at odds with the morphological diversity of aquatic particles (Dusenbery 1998; Clavano et al. 2007; Guasto et al. 2012; Conley and Sutherland 2017).

The hydrodynamics of particle capture in ascidians remain vague and descriptions of particle capture in the branchial sac are primarily from the older literature (Orton 1913; Jørgensen 1949; Erika and Werner 1954; Millar 1971). In this study, we sought to investigate the hydrodynamics of ascidian filtration and the process of particle capture using video endoscopy and direct sampling of differently-shaped polystyrene particles in the inhaled and exhaled water. Specifically, we addressed the following research questions: (1) Do ascidians filter using aspects of cross-flow filtration? (2) Does particle shape affect interactions with the fluid and mesh? (3) As a consequence of (2), is particle shape (and also size) a major determinant of capture efficiency?

Methods

Animal collection and husbandry

Direct sampling of particle capture was conducted using *S. plicata* ($N = 12$) that were collected from ropes and chains at Jaffa Harbor, Israel. Animals were quickly transported to The School of Marine Sciences in Mikhmoret, Israel, secured in a cup of gravel, and kept in a sea table with running seawater at ambient temperature of 28 °C and salinity of 39–40 PSU. Once a day the water flow was stopped for an hour and the ascidians were fed with fresh algae (*Nannochloropsis* sp., ~ 10^6 algal cells per beaker). A subsample of *Nannochloropsis* was filtered onto a 0.2 µm polycarbonate membrane, imaged using an epifluorescence microscope (BX53, Olympus), and size measurements were determined using ImageJ (NIH, USA). Endoscopy was conducted on *H. momus* collected by SCUBA divers from ropes of the Sea Bream Farm off the coast of Mikhmoret at ~ 5–18 m depth (N32°24.700′, E034°50.250′). All ascidians were fed

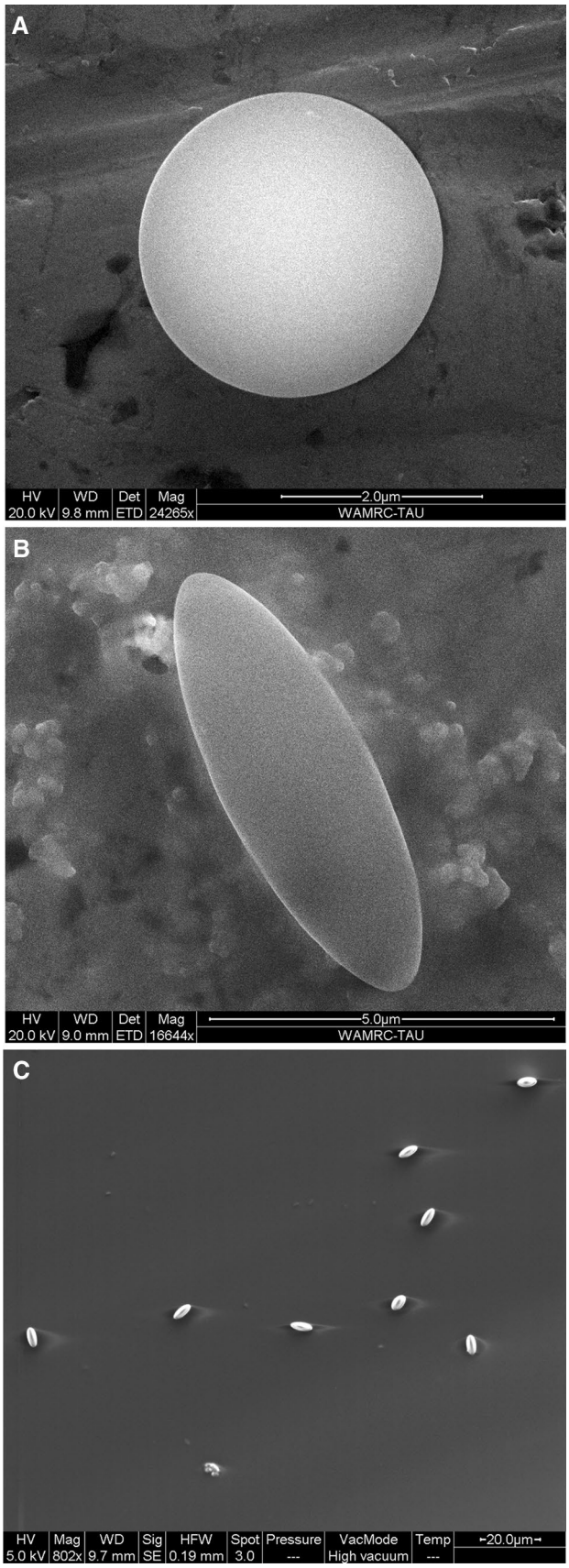

Fig. 2 Scanning electron micrographs of polystyrene microparticles. ▶ **a** Unstretched microspheres and **b**, **c** stretched microellipsoids, showing that the stretching procedure creates uniform particles and does not alter the surface structure of the particles

cultured *Nannochloropsis* sp. a few hours before direct sampling or endoscopic examination to stimulate secretion of the mucous mesh. Endoscopy was performed within 3 days to 3 months of animal collection.

Dye visualization studies were performed using *C. intestinalis* collected by the Marine Resource Center, Woods Hole, MA. *Ciona intestinalis* was chosen for dye visualizations because of its semi-transparent tunic.

Experimental particles

To test the effect of particle shape on capture efficiency, ellipsoidal microparticles (hereafter referred to as "microellipsoids") were synthesized using a toluene-stretching method (Ho et al. 1993; Champion et al. 2007; Conley and Sutherland 2017). Briefly, spherical polystyrene microparticles (Polysciences Fluoresbrite® YG carboxylate microspheres, 486 nm emission) were embedded in a polyvinyl alcohol (PVA) film and mounted on a custom-built stretching device. The stretcher was immersed in a toluene bath for 3 h to partially dissolve the polystyrene microspheres, and then the PVA film was stretched twofold to elongate the particles. The PVA film was then left overnight for particles to re-solidify, and then the PVA was dissolved in water to re-suspend the microellipsoids. Control spherical microparticles (hereafter referred to as "microspheres") were treated with the same toluene bath procedure but the PVA film was not stretched. Microellipsoids used for direct sampling of capture efficiency had a mean length and width of 0.7 ± 0.4 and 0.3 ± 0.3 µm, respectively ($N = 21$; mean ± SD).

The effect of stretching on the surface rugosity of particles was confirmed by visualizing microellipsoids using a scanning electron microscope (SEM). Samples were prepared by placing a 5 µL drop of the solution of microellipsoids onto a freshly-cleaved piece of silicon and fixed onto an aluminum stub using double-sided carbon tape. SEM images were obtained using an FEI Quanta 200F SEM scanning electron microscope at 5.0 and 20 kV in high vacuum mode. Both microspheres and microellipsoids had smooth, featureless surfaces (Fig. 2a, b), and the microellipsoids showed no signs of alterations from the stretching procedure other than shape (Fig. 2b, c).

Hydrodynamics and mesh movement

Visualizations of the organismal-scale flow structure were performed using Disodium-fluorescein dye (Fisher Scientific, #S25328) mixed with seawater. The dye was gently

ejected from a micropipette a few millimeters upstream of the inhalant siphon of the semi-transparent ascidian *C. intestinalis* (inhalant siphon diameter: 0.3 cm; length: 1.7 cm) in the laboratory.

Endoscopic examinations of mesh-scale flow patterns and mesh-particle interactions were conducted using a rigid borescope with HOPKINS rod lens optical system (Karl Storz, viewing angle: 30°; field angle: 40°; outer diameter: 1.9 mm; working length: 100 mm). Three different cameras were used at different times throughout the experiment: (1) a Telecam camera head connected to a Telecam DX II Camera Control Unit (720 × 480 pixel resolution), (2) an iPhone 5S (1080 × 1920 pixel resolution), and (3) an iPhone 5 SE (2160 × 3840 pixel resolution), the latter two with a SmartScope adapter (Karl Storz CAT #202882I6) mounted directly to the endoscope. For all setups, the endoscope was equipped with an adjustable Techno LED Nova 150 cold light source (Karl Storz, up to 180 W) and was mounted on a MM-33 micromanipulator (Sutter Instrument) that was positioned above the ascidian on a solid stand. The optical insertion tube (OIT) was lowered gently into the inhalant siphon of the ascidian and video recording was initiated when both siphons were open and the animal appeared relaxed. No "densensitization" of animals to the OIT was performed (Armsworthy et al. 2001). Recording speed for all videos was 30 frames s^{-1}. Fluorescent microspheres (20 µm) were used to calibrate the spatial scale.

A high concentration of yellow-green fluorescent 0.5 µm microspheres (486 nm emission) was used to visualize the mucous mesh (~ 10^8 microspheres mL^{-1} added to inhalant siphon) of *H. momus*. Videos for measurements of mesh speed were taken from the dorsal side of the animal at the posterior portion of the branchial sac, an area that provided views of the mesh moving in a single plane.

Visualizing the capture process of microellipsoids

Three sizes of fluorescent microellipsoids (4.5 × 13, 8 × 22, 15 × 44 µm) were each observed pre- and post-capture on the mesh of *H. momus* using endoscopy. Microellipsoids were vortexed and then gently injected directly above the inhalant siphon using a pipette. Each size of microellipsoid was applied and observed separately. Observations of microellipsoid capture were collected from the endostyle side because particle capture was observed there more frequently.

Direct sampling of particle capture efficiency

We used a direct sampling method (Wright and Stephens 1978) coupled with flow cytometry to quantify particle concentrations and calculate the filtration efficiency of differently-shaped microparticles captured via hydrosol filtration. We compared the capture of 0.3 µm (± 0.01 µm SD) microspheres, 0.3 ± 0.3 × 0.7 ± 0.4 µm microellipsoids, and 1.0 µm (± 0.01 µm SD) microspheres of identical material. Ascidians in gravel cups were placed individually in 1 L Pyrex beakers with the water supply turned off. Small tubing (PTFE tube, 60–90 cm long, ID 400 µm, outer diameter 800 µm) was inserted carefully a few mm into the ascidians' siphons and used to simultaneously sample the inhaled and exhaled water. Prior to the addition of artificial microparticles, *Nannochloropsis* was added and a sample was collected to establish normal feeding behavior (data not shown). The beaker was then flushed with fresh seawater, and a mixture of *Nannochloropsis* and the fluorescent microparticles of each treatment type were slowly syringe-injected into the beaker. In vivo fluorometry (AquaFluor, Turner Design) was used to determine that a similar concentration of *Nannochloropsis* (10^2–10^4 cells mL^{-1}) was applied to each treatment. Samples were collected into 2 mL Eppendorf tubes by slow gravity siphoning at a rate of 0.2–0.4 mL min^{-1} (see Jacobi et al. 2017 for a detailed description). Since the microparticles are similar in density to seawater (1.05 g cm^3) and sampling was short (~ 5 min), stirring was not necessary to keep microparticles suspended. Each sample was fixed with 50% analytical grade glutaraldehyde (final concentration 0.1%) and kept at 4 °C until analysis with flow cytometry.

The difference in particle concentrations between a pair of samples provided a direct measure of the capture, and capture efficiency was calculated as $CE = \frac{C_{in}-C_{ex}}{C_{in}}$, where CE is the capture efficiency, and C_{in} and C_{ex} are the concentrations of a certain particle group (e.g. size group) in the inhaled and exhaled water, respectively.

Since preliminary trials showed that the capture efficiency of a single particle type varied temporally for a single animal, repeated measurements were made for each animal. Previous work with *S. plicata* showed > 70% capture efficiency of *Nannochloropsis* and 1.0 µm microspheres in the lab (Jacobi et al. 2017). Therefore, samples in which *Nannochloropsis* were captured below 70% were omitted from further analysis based on the assumption that the animals were not feeding constantly throughout the sampling period. Forty-six out of 61 samples met this quality criterion, capturing algae above 70%; the remaining 15 samples were excluded from analysis.

Flow cytometry

Inhalant and exhalant samples were analyzed fresh using an Attune Acoustic-Focusing Flow Cytometer (ThermoFisher Sci.). Microspheres and microellipsoids were analyzed based on forward scatter versus green fluorescence using violet laser excitation (405 nm). *Nannochloropsis* was analyzed based on forward scatter vs. red fluorescence using 488 nm laser excitation. To ensure reliable quantification of all size

groups, the event rate was kept below 600 events s^{-1} by setting the flow rate to either 25 or 100 µL min^{-1}. See Jacobi et al. (2017) for a detailed description.

Since the forward scatter signal of the 0.3 µm microspheres could not reliably be differentiated from that of the microellipsoids, the 0.3 µm microspheres were always applied separately from the microellipsoids in the direct sampling. Only microparticles that appeared as singlets (based on the combination of forward scatter and green fluorescence signal) were gated and quantified.

Particle tracking

Recorded videos from the endoscope were converted using QuickTime Pro (Apple) to an image stack that was analyzed in ImageJ (NIH, USA) for measurements of velocity, particle orientation, and morphometry. Particle tracking velocimetry for mucous mesh speeds and free-stream velocities was done by manually tracking individual microparticles between frames using the plugin MTrackJ (Meijering et al. 2012). To test whether ascidians filter by dead-end sieving, we analyzed the incident angle at which microparticles approached the filter prior to capture. Incident angles and microellipsoid orientations were both measured using the straight line angle tool in ImageJ (Schneider et al. 2012). Microellipsoid orientations were measured relative to the fluid flow (0°), while the incident angle at which particles approached the filter was measured using the anterior–posterior angle of the branchial sac as the reference point (0°) (Fig. 1f). Since many particle trajectories curved directly prior to capture (1–5 frames), orientations were measured during both the straight period of the trajectory (i.e., the first point of particle appearance in the field of view and the last point of the trajectory prior to any curvature) and during the period of curvature (hereafter referred to as the angle pre-curvature and the angle of approach, respectively) (Fig. 1f).

Statistical analysis

Capture efficiency data was analyzed using R (R Core Team 2013). Since multiple measurements of capture efficiency (2–7) were obtained from each individual, average capture efficiency for each individual was analyzed statistically as paired samples with a balanced design. Three negative values of capture efficiency (− 2 to − 15%) were converted to zeroes prior to statistical analysis on the basis that negative capture efficiencies reflect the limited precision of the flow cytometer rather than a real biological signal. The particle capture efficiency of *S. plicata* was left-skewed and violated the assumptions for a repeated-measures ANOVA. Transformations did not homogenize the variance, so the capture efficiency of different particle types was tested using the nonparametric equivalent of a repeated measures ANOVA (Friedman's test), followed by a Nemenyi test for pairwise multiple comparisons. We used G*Power software (version 3.1.9.2) to perform post hoc statistical power analysis, assuming a medium effect size of 0.3 and an error probability α of 0.05 to calculate power ($1 - \beta$) (Cohen 1988).

Data on the orientation of ellipsoidal particles were collected on a 0°–90° scale, with 0° representing a microellipsoid oriented parallel to the direction of flow. Throughout the manuscript, values are reported as mean ± 95% CI unless stated otherwise.

Results

Hydrodynamics and mesh movement

Dye visualizations of organismal-scale flow patterns in the branchial sac of *C. intestinalis* showed flow was laminar. Sieving (i.e., flow perpendicular to the mesh) occurred predominantly on the exhalant siphon side rather than homogenously across the entire branchial sac (Fig. 3, Supplementary video 1). Flow moved vertically down the branchial sac—parallel with the mesh—in both the anterior–posterior directions and ventral-dorsal directions (Fig. 3, Supplementary video 1). Observations from dye visualizations were used to inform the schematic depictions of flow patterns shown in Fig. 1c, e.

Visualization of flow in the branchial sac of *H. momus* using fluorescent microellipsoids (4 × 13 µm) as a tracer showed that flow tens of micrometers away from the mesh was parallel to the mesh (Figs. 1f, 4; Supplementary video 2). The mean particle speed prior to particle capture was 0.55 ± 0.19 mm s^{-1} ($n = 89$ velocity tracks from 5 microparticles, $N = 2$ animals). Particle capture was identified based on the abrupt change in the trajectory and speed of the particle upon adhesion to the mesh (Fig. 5, Supplementary video 2). Particles decelerated prior to encountering the mesh, presumably due to the boundary layer at the mesh, and then, once adhered to the mesh, traveled laterally along the interior wall of the branchial sac (Fig. 5). Prior to capture (0.07–0.2 s), particles curved toward the filter (Figs. 4, 5). The mean particle speed slowed to 0.36 ± 0.39 mm s^{-1} 0.1 s prior to capture ($n = 14$ velocity tracks from 28 microparticles, $N = 3$ animals). The mean angle of the particle arrival trajectory (relative to branchial sac, 0°) prior to curvature was 3 ± 1° ($n = 48$ microparticles, $N = 2$ animals), while the mean angle of approach was 32 ± 3° ($n = 45$ microparticles, $N = 2$ animals) (Fig. 4).

Microparticles in the inhalant water near the endostyle traveled in a posterior direction. In one case, microellipsoids came into close proximity to the mesh but 72% (18 out of 25) of the particles in the field of view did not appear to be captured on the mesh but rather accelerated (1.4 ± 0.69 mm s^{-2},

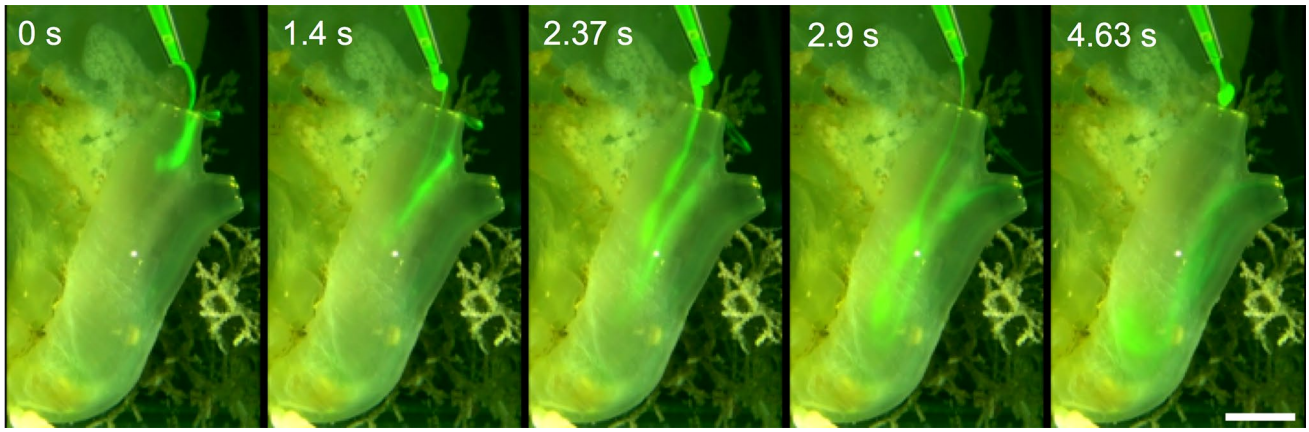

Fig. 3 Time-lapse photographs taken from video of fluorescein dye gently ejected by a micropipette into the inhalant siphon of a semitransparent *Ciona intestinalis*, showing the flow patterns in the branchial sac. Scale bar 1 mm

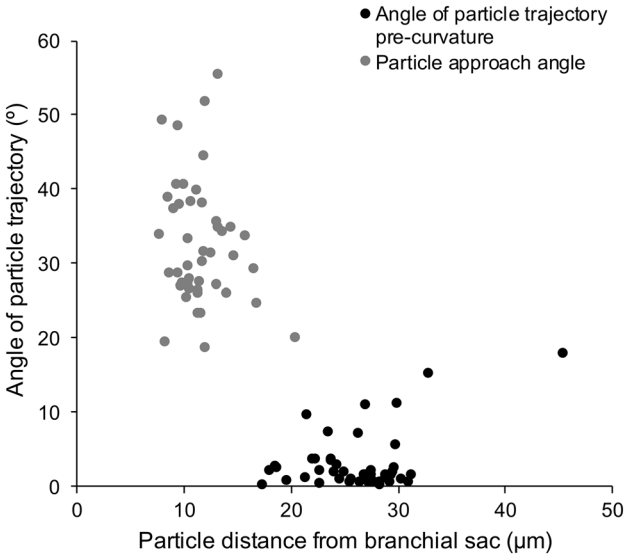

Fig. 4 Angles of the pre-capture trajectories of 4.5 × 13 μm microellipsoids near the endostyle pre-curvature (Φ_t, where branchial sac = 0°) and the angle as the particle approaches the mesh (particle approach angle, Φ_a). See text and Fig. 1f for details

$n = 10$ microparticles, $N = 1$ animal) on a downward trajectory toward the bottom of the branchial sac (Supplementary video 3), carried posteriorly by the parallel crossflow component.

We were able to indirectly visualize the behavior of the mucous mesh by observing the intercepted particles. Particles caught on the mucous mesh moved uniformly along the branchial wall at a much slower speed than particles in the fluid (Table 1, Fig. 5) and did not flow out the stigmata (Supplementary video 4 shows 20 μm microspheres traversing the mesh). Although the mean mesh speed was consistently between 0.1 and 0.2 mm s^{-1} across individuals (Table 1), an individual's mesh speed varied by a factor

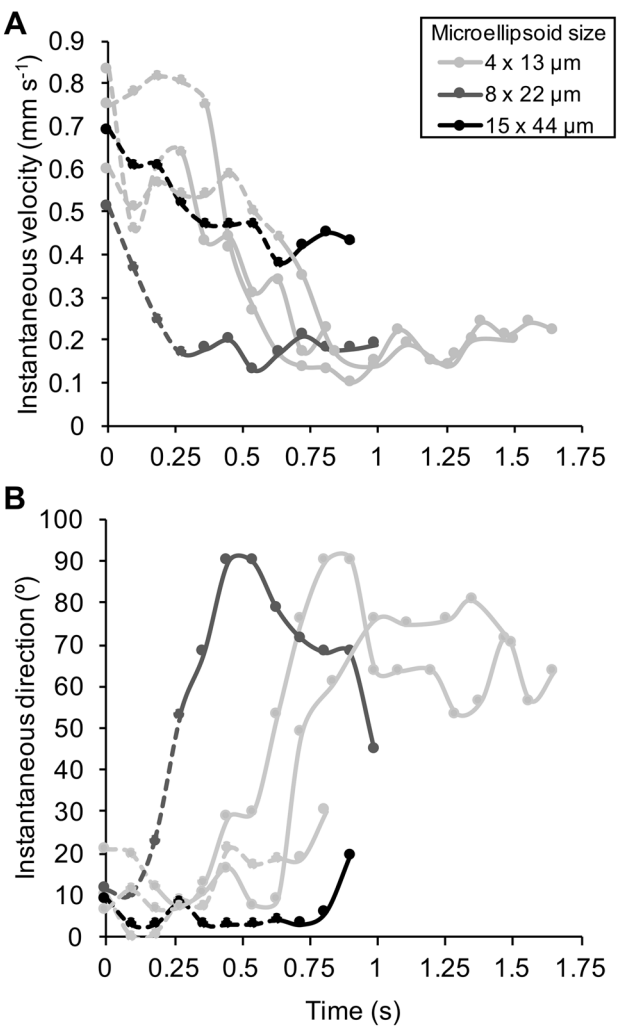

Fig. 5 **a** Speed and **b** direction of five microellipsoids (relative to the fluid direction, 0°) pre-capture (dashed segment of the line) and post-capture (solid segment of line) on the mesh of *Herdmania momus*. The precision of speed and direction measurements is ± 3 frames or 9.9%

Table 1 Measurements of mesh and free-stream fluid speeds determined from endoscopy in *Herdmania momus*

Individual	Mesh speed, mm s^{-1} mean ± 95% CI (range)	*N*, *n*	Fluid speed, mm s^{-1} mean ± 95% CI	*N*, *n*
1	0.20 ± 0.05 (0.05–0.33)	14, 126	1.5 ± 0.4	10, 63
2	0.17 ± 0.05 (0.05–0.41)	14, 147	2.4 ± 0.7	5, 37
3	0.12 ± 0.04 (0.04–0.17)	6, 110	0.62 ± 0.1	7, 174
4	0.10 ± 0.04 (0.03–0.18)	8, 79	1.7 ± 1.0	6, 79
Total	0.15 ± 0.07 (0.03–0.41)	4	1.6 ± 1.2	4

For consistent comparisons, all measurements were obtained using 10 or 20 µm microparticles as tracers with the optical insertion tube of the endoscope placed in the dorsal lamina area at the lower part of the branchial sac, where the mesh is assumed to be fully stretched

N is the number of independently measured microparticles, *n* is the total number of instantaneous velocities measured

CI is confidence interval for the mean

of 2–10. During the same filming session for ascidian 2, the mesh speed increased from 0.04 to 0.41 mm s^{-1} after the addition of 10 µm microspheres. Mucous mesh conveyance along the branchial sac could also stop temporarily and then resume. Although we did not attempt to directly test the potential for an active behavioral response to particle loads, it is evident that the ciliary transport speed of the mucus can vary, at least for short periods of time.

The mean free-stream fluid velocity in the branchial sac of *H. momus* was 1.5 mm s^{-1} (Table 1), which is comparable to measurements made at the inhalant siphon of *C. intestinalis* using particle image velocimetry (0.4–3.8 mm s^{-1}) (Du Clos 2016). Based on the characteristic length scale of the diameter of the inhalant siphon of *H. momus* (11 ± 1.3 mm, $N = 5$), the average free-stream fluid velocity (1.5 mm s^{-1}), the dynamic viscosity of seawater (9.08 10^{-4} kg m^{-1} s^{-1} at 28 °C), and the density of seawater (1.026 10^{3} kg m^{-3} at 28 °C), the Reynolds number for the fluid of the branchial sac is ~ 20. Based on the characteristic length scale of a single filter fiber (diameter ~ 10 nm, Flood and Fiala-Medioni 1981) and the average pre-capture particle approach speed (0.36 mm s^{-1}), we calculated the Reynolds number for ascidian filtration to be 4×10^{-6}, which is consistent with our observations from dye visualizations in the branchial sac that showed laminar flow.

At high enough particle concentrations using fluorescent 0.5 µm microspheres, the mucous mesh became visible (Fig. 6a), allowing us to observe the mesh behavior in addition to the particle trajectories. Contraction of the animal, often in response to disturbance from the OIT or high particle concentrations, caused the movement of the mesh along the branchial sac to cease, or detached the mesh from the branchial sac (Fig. 6b) (Supplementary video 5). This behavior was not observed in actively filtering animals at low particle concentrations.

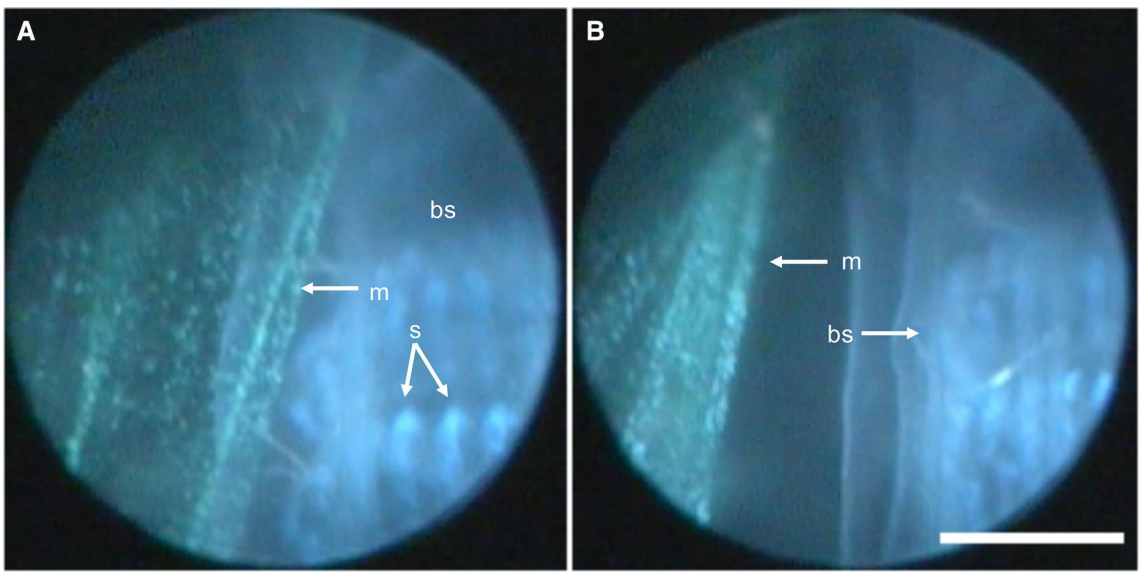

Fig. 6 Endoscope micrographs of the mucous mesh on the branchial sac of *Herdmania momus* (Supplementary video 5). **a** Mucous mesh (*m*) visualized using 0.5 µm fluorescent green microspheres. Mesh shown traversing branchial sac (*bs*) prior to a contraction. *s* stigmata. **b** Mucous mesh detached from a fold of the branchial sac during contraction. Scale bar 0.1 mm

Table 2 Orientation relative to the fluid streamlines of three sizes of microellipsoids in the fluid of the branchial sac (pre-capture) and on the mucous mesh (post-capture) of *Herdmania momus*

Location	Microellipsoid dimensions (μm)	Mean orientation (°)	Variance (°)	Standard deviation (°)
Fluid	4 × 13	10	7	0.4
Fluid	8 × 22	8	8	0.5
Fluid	15 × 44	16	2	17
Mesh	4 × 13	34	4	22
Mesh	8 × 22	45	6	27
Mesh	15 × 44	34	5	24

Visualizing the capture process of microellipsoids

Using endoscopy, we were able to observe the capture process of microellipsoids by *H. momus*. All sizes of microellipsoids in the fluid of the branchial sac oriented with their long axes parallel with fluid streamlines, regardless of the ellipsoid size (Table 2, Fig. 7). Ellipsoids approached the mesh with their short axes toward the mesh, and upon contact with it, they reoriented to lie flat with the long axes on the mesh (Supplementary video 6, 10 fps). Post-capture, microellipsoids oriented ~ 35°–45° relative to the fluid streamlines, with the long axes roughly oriented with the direction of mesh movement (Table 2). The mean orientation angle in the fluid and on the mesh was similar across all three sizes of microellipsoids (Table 2).

Direct sampling of particle capture efficiency

Cultured *Nannochloropsis* cells were approximately spherical, ~ 2 μm (length = 2.1 μm ± 0.24, width = 1.9 μm ± 0.19, $N = 6$). Using the capture of *Nannochloropsis* by *S. plicata* as a quality control indicator of normal feeding behavior, we were able to detect that the capture patterns for the same individual could vary with sampling (Fig. 8). For example, in individual 6, the capture efficiency of ellipsoidal particles varied from 27 to 82%, while the capture efficiency of *Nannochloropsis* was 98 and 99% for the respective samplings (Fig. 8). Likewise, individual 1 captured 1.0 μm microspheres with 98% efficiency while capturing *Nannochloropsis* with only 73% efficiency, but at another sampling captured 1.0 μm microspheres with 59% efficiency and *Nannochloropsis* with 100% (Fig. 8). The average of the repeated measurements of the capture efficiency of *Nannochloropsis* was 90 ± 2% ($N = 12$) (Fig. 9).

Particle type (size and shape) significantly affected the average capture efficiency of *S. plicata* (Friedman $\chi^2 = 26.9$, $df = 3$, $P < 0.001$). *Nannochloropsis* and 1.0 μm microspheres were both captured with high efficiency (86 ± 10% for 1.0 μm microspheres), with no significant difference between the two ($P = 0.96$, Nemenyi test, Power = 0.39, critical $\chi^2 = 7.8$) (Fig. 9). Microellipsoids were captured with significantly lower efficiency than *Nannochloropsis* and 1.0 μm microspheres ($P = 0.002$ and $P = 0.009$, respectively), as were 0.3 μm microspheres ($P = 0.002$ and $P = 0.002$, Nemenyi test). The capture of microellipsoids (32 ± 26%) was not statistically different from that of the 0.3 μm microspheres (31% ± 27%, $P = 0.96$, Power = 0.39, critical $\chi^2 = 7.8$); however, the microellipsoids had a somewhat higher maximum average capture efficiency (76%) than the 0.3 μm microspheres (68%). The capture efficiency of both 0.3 μm microspheres and microellipsoids was more variable than capture of 1.0 μm microspheres (Fig. 9).

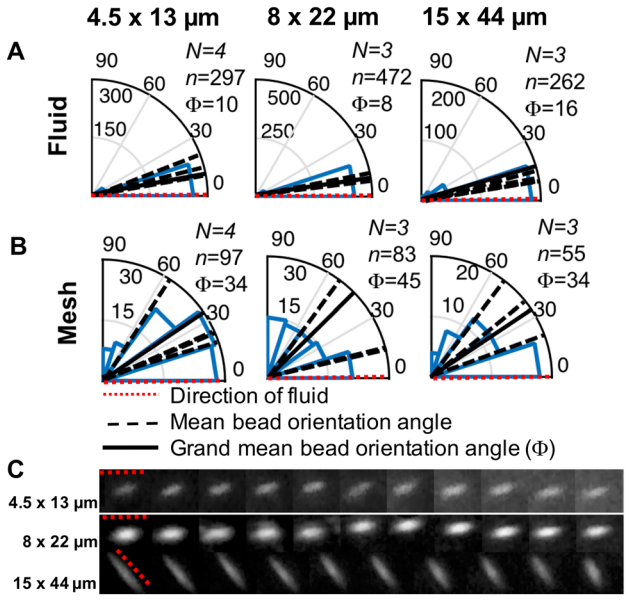

Fig. 7 Orientation of three sizes of microellipsoids (4.5 × 13, 8 × 22, 15 × 44 μm) in the fluid near the branchial sac and on the mesh of *Herdmania momus*. **a** Frequency histograms showing the orientation angles of microellipsoids in the fluid of the branchial sac. **b** Frequency histograms showing the orientation angles of microellipsoids on the mucous mesh. All angles are relative to the fluid flow (i.e., direction of fluid flow = 0°). The area of each sector is proportional to the frequency in the corresponding angle group. Dashed black lines show the mean for each individual animal, solid black line shows the overall mean (*Φ*). *N* signifies number of individual ascidians from which observations were obtained; *n* signifies the total number of observations (angles measured in **a**, microellipsoids tracked in **b**). **c** Image sequences show sample microellipsoid trajectories in the fluid near the branchial sac. Time between frames is 0.03 s. Red dotted line indicates the direction of the fluid

Discussion

Collectively, our results suggest that the depiction of ascidians as continuous, non-selective direct sieves does not reflect the behavioral and hydrodynamic complexity of

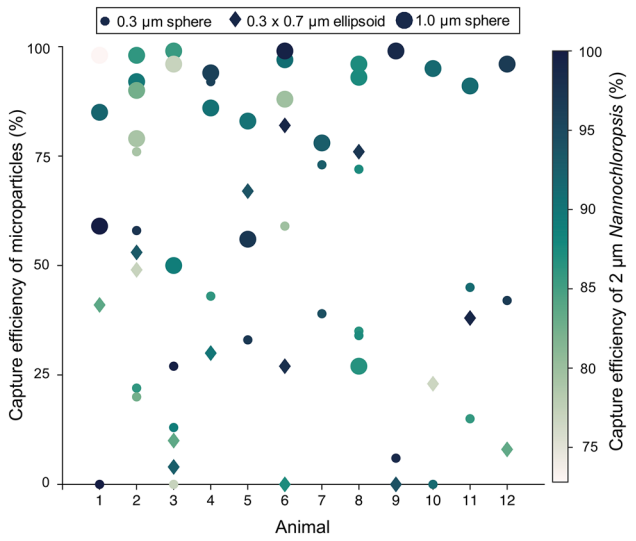

Fig. 8 Repeated measures of the capture efficiency of *Styela plicata* fed microspheres, microellipsoids, and *Nannochloropsis,* showing variability of capture patterns within and between individuals. Measurements were obtained through direct sampling of the water inhaled and exhaled by ascidians in the laboratory. Capture efficiency of *Nannochloropsis* was used as an indicator that animals were feeding normally, since based on its size (~ 2 µm) it should be captured at or above 70% based on results from a previous study on the retention efficiency of *Styela plicata* using the same method (Jacobi et al. 2017)

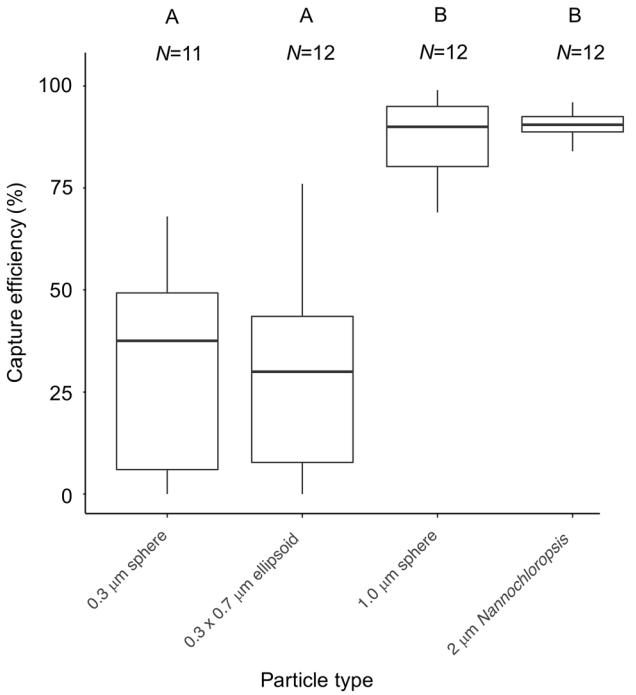

Fig. 9 Capture efficiency of different sized and shaped particles by the ascidian *Styela plicata*. Measurements were obtained through direct sampling of the water inhaled and exhaled by ascidians in the lab. In the boxplots, the box top and box bottom represent the first and third quartile, respectively; the horizontal line in the box shows the median; whiskers show the range. Any groups sharing the same letter are not significantly different based on Nemenyi post hoc test ($\alpha = 0.05$)

ascidian feeding. Previous schematic representations of flow in the branchial sac of ascidians (Erika and Werner 1954; Alexander 1981; Jørgensen et al. 1984; Pennachetti 1984; Petersen 2007) (Fig. 1d) oversimplify the different spatial scales of flow patterns. The capture efficiency of small particles (≤ 1 µm) can vary widely for an individual animal even when larger particles are captured at high efficiency (Fig. 8). Mesh secretion is not always continuous, and an individual's mesh speed can also change on very short time scales (Table 1).

Hydrodynamics and mesh movement

Ascidians adhere to the sieving model in that pressure differences move all of the feed through the filter, filtered particles adhere to the filter (Fig. 6), and *Nannochloropsis* (~ 2 µm), which is larger than the mesh pores, were captured with an average efficiency of 90% (Fig. 9). However, ascidian filtration also shares some hydrodynamic similarities with crossflow filtration (Fig. 1b, e). Structurally, ascidians resemble a tubular membrane crossflow filtration system where the filter is on the inside wall of the tube. There is a "crossflow" component in the branchial sac, where the fluid being filtered is pumped along the surface of the mesh rather than exclusively perpendicular to it (Fig. 1e, f), but the crossflow velocity is evidently insufficient to prevent all particles from contacting the mesh. These results indicate that ascidians filter using aspects of crossflow (tangential) filtration, and we suggest that ascidian filtration acts as a hybrid-flow filtration system rather than a classical direct sieve. Although the tubular morphology of ascidians seems to necessitate some parallel flow, we could find no prior studies that have previously described flow in the branchial sac to be tangential to the mucous mesh.

Endoscopic observations with bivalves showed similar crossflow fluid motion over the gill of the mussel *Mytilus edulis,* with an approximately 30° angle of approach to the ctenidial plane (Ward et al. 1998, 2000). Models and microscopic observations with *M. edulis* showed that flow in the posterior portion of the mussel gill becomes more normal to the gill surface with steeper particle approach angles (70°–90°) tens to hundreds of micrometers away from the ctenidia (Riisgård and Larsen 2000; Ward et al. 2000). Particle trajectories close to the ordinary gill filaments of scallops (*Aequipecten opercularis*) also can be parallel to the long axis of the gill (Riisgård and Larsen 2005). Our results suggest that the near-filter flow in ascidians is more parallel to the filter surface than that of bivalves (Fig. 4); it is important to acknowledge, however, that such measurements are inherently sensitive to the angle of observation, as well as

the temporal and spatial scale under consideration (Riisgård and Larsen 2000). Our measurements of capture trajectories were viewed from the side of the branchial sac (Fig. 1f). From this angle, the particle approach angle was consistently parallel to the filter, even tens of micrometers from the mesh, and the curvature of the trajectories was ~ 30° at ~ 10 µm from the mesh (Fig. 4). Because of the pressure drop across the filter, the near-field flow may become more orthogonal to the mesh at spatial and/or temporal scales smaller than the resolution of our video endoscopy system, but if so, this transition appears to occur on smaller spatial scales than those in bivalves. We also cannot exclude the possibility that the presence of the OIT of the endoscope could have altered the trajectories and angles of some particles within the branchial sac; however, the diameter of the OIT (1.9 mm) is small relative to the diameter of the inhalant siphon of *H. momus* (~ 10 mm), and nonintrusive dye visualizations support endoscopy observations of flow patterns.

Some authors have previously acknowledged that many animals use filters whose fibers are not oriented normal to the direction of flow (Rubenstein and Koehl 1977; Braimah 1987), and that this affects both the efficiency of particle capture via hydrosol mechanisms and the pressure drop of the filter (Spielman and Goren 1968). Two factors influence the optimum function of a biological feeding-filter: (1) high contact with edible particles and (2) low resistance to flow (Vogel 1994). These criteria are usually opposing because fine-meshed filters, such as those used by ascidians, have a high resistance to flow (Vogel 1994). While a strictly sieving filter is subject to excessively high pressure drop and high clogging rates (Chen 1955), bulk flow parallel to the mesh offers several advantages in terms of resistance. Cylindrical filter fibers in parallel flow experience less drag (Vogel 1994) and a lower pressure drop (Chen 1955) than those subjected to normal flow, lowering the energetic cost of filtration.

One prior study used endoscopy to observe ascidian feeding (Armsworthy et al. 2001). These experiments described the feeding process of *H. pyriformis* during exposure to low and high particle concentrations. Two distinct feeding modes were observed: one, at low particle concentrations, in which the mucous mesh traversed the entire surface of the branchial sac (crest and folds) in the classically described manner, and a second, at high particle concentrations or sediment loads, when squirting turned the mucous mesh into strands that traversed solely the crests of the sac. These two modes occurred at significantly different speeds—a fast (0.074 mm s^{-1}) and slow speed (0.015 mm s^{-1}). Another study used a dissected window in the tunic to observe mucous mesh behavior of *Ascidia paratropa* and found that the mesh could detach from the surface of the branchial sac, moving as a flat sheet from the endostyle to the dorsal lamina through the "pulling" of the dorsal lamina rather than by the cilia of the stigmata (Pennachetti 1984). This form of mucus transport was reportedly often associated with high concentrations of particulate material and prior to the animal squirting (Pennachetti 1984). Our observations of the detachment of the mucous mesh from the branchial sac (Fig. 6b) at high particle concentrations appear quite consistent with this description provided by Pennachetti (1984). However, because we only observed this behavior when animals were fed a very high concentration of 0.5 µm latex microspheres (~ 10^8 microspheres mL^{-1}), we do not consider it a component of undisturbed feeding behavior. Nonetheless, it may play a role during exposure to high sediment loads from episodic events such as storms and storm-water runoff (Ali and Tamilselvi 2016), as suggested by Armsworthy et al. (2001).

The transport speed of the mucous mesh influences the exposure time of the mesh and hence the amount of water filtered through each area of the filter. The speed of ascidian mesh transport may vary with species or animal size (Flood 1982), particle concentration (Armsworthy et al. 2001), and likely with temperature, since it affects the viscosity of the water and mucus and the beating speed of cilia (Flood 1982). Variation in mesh speed may also be caused by an increased rate of secretion from the endostyle, or by stretching the mesh through pulling by the dorsal lamina. Previous studies have reported ascidian mesh speeds ranging from 0.015 to 0.22 mm s^{-1} (Flood 1982; Armsworthy et al. 2001). Our measurements of the mean mesh speed fall within the upper boundary of this range and reveal a faster upper limit (0.41 mm s^{-1}) for mucous mesh transport (Table 1). Variation in mesh speed could indirectly contribute to the different capture patterns observed within individuals (Fig. 8)—faster mucus transport speeds would lower exposure time of the mesh and lessen the likelihood of clogging, or rapid pulling of the mesh could effectively stretch the mesh pores.

Visualizing the capture process of microellipsoids

Ellipsoidal particles oriented non-randomly in both the fluid of the branchial sac and post-capture on the mesh (Table 2, Fig. 7), indicating that particle shape affects interactions with the fluid and mesh. Endoscopic observations of microellipsoid capture by *H. momus* revealed that the minimum axis of the ellipsoid is intercepted by the filter fiber (Supplementary video 6), thereby providing the mechanism for the capture patterns found through direct sampling of *S. plicata*. These results are consistent with those from appendicularians (Conley and Sutherland 2017), copepods (Visser and Jonsson 2000), and carp larvae (Drost et al. 1987). The behavior of ellipsoidal prey thus appears consistent across predator feeding structures, and our work extends the applicability of these mechanisms from planktonic consumers to a benthic suspension-feeder.

The measured speed of ellipsoidal particles in the 0.1 s prior to particle capture (0.36 ± 0.39 mm s^{-1}) is consistent with previous calculations of flow velocities through the filter based on the pumping rate at zero back pressure (0.2–0.37 mm s^{-1}) (Jørgensen 1983; Jørgensen et al. 1984; Riisgård 1988; Petersen 2007).

Direct sampling of particle capture efficiency

Our direct sampling results show nearly 100% capture of particles > 1.0 µm and intermediate capture efficiency of 0.3 µm particles (Fig. 9). While dead-end sieving predicts 100% capture of particles larger than the mesh pores and 0% capture of particles smaller than the mesh pores, hydrosol filtration predicts some capture efficiency of particles smaller than the mesh pores (Rubenstein and Koehl 1977). Our results suggest hydrosol mechanisms add to particle capture by ascidians, consistent with Jacobi et al. (2017). Hydrosol mechanisms have been shown to contribute to capture of small particles by salps and appendicularians (Deibel and Lee 1992; Acuña et al. 1996; Fernández et al. 2004; Sutherland et al. 2010; Kiørboe 2011), but such mechanisms have not been as well documented for ascidians until recently (Dadon-Pilosof et al. 2017; Jacobi et al. 2017). Previous studies have suggested that ascidians can only capture particles down to 1–2 µm with 100% efficiency, but the lower size limit of efficient capture is not universally agreed upon (Jørgensen et al. 1984). A review of ascidian suspension feeding asserted that there are no studies demonstrating capture of submicrometer particles, and that if submicrometer particles are captured, they cannot constitute a quantitatively important food source (Petersen 2007). Endoscopic observations showed that 0.5 µm microspheres were effectively captured on the mesh of *H. momus* (Fig. 6), and we did not observe any 0.5 µm microspheres flowing through the mesh, even at lower particle concentrations. Although 0.3 µm microspheres could not successfully be visualized by the endoscope, results from direct sampling with *S. plicata* (Fig. 9) indicate that capture of particles < 1.0 µm occurs through hydrosol mechanisms, as previously suggested (Dadon-Pilosof et al. 2017; Jacobi et al. 2017). These observations support the notion that ascidians have a very fine mucous mesh that is able to efficiently capture prey the size of solitary bacteria.

The application of aerosol filtration theory to biological filters revolutionized our understanding of the mechanisms for size-selective feeding (Riisgard and Larsen 2001). The theory's assumption of spherical prey particles (Rubenstein and Koehl 1977) is nonetheless at odds with the wide-ranging morphologies of aquatic particles: bacteria range from coccoid to bacillocid to vibrioid; flagellates are often asymmetrical, with spines, scales, or collars; diatoms encompass filamentous, pennate, centric, and discoid forms. Our results show how the length-to-width ratio of particles affects particle-encounter efficiency through hydrosol capture mechanisms: the minimum diameter of ellipsoidal particles determines the capture efficiency (Fig. 9). These results indicate that particle shape and size determine the capture efficiency, and that ellipsoidal particles may be appropriately modeled as spheres of equivalent minimum diameter for capture efficiency predictions.

Concluding remarks

Further work examining the flow fields of the entire branchial sac would enhance our understanding of ascidian filtration. For example, the possibility of recirculation in the branchial sac has not been explored. Flow in the pharyngeal filter of salps has been observed to be circular, and such flows may serve to concentrate particles via recirculation (Sutherland 2010; Sutherland et al. 2010), similar to the role of the food-concentrating filter of appendicularians (Morris and Deibel 1993). In describing ascidian feeding, Jørgensen (1949) stated "a certain amount of aggregated particles was always observed when the [filtered] suspensions were examined under the microscope", suggestive of a possible role of recirculation and concentration in the branchial sac. Video observations and dye visualizations of the fine filtering combs of the cladoceran *Daphnia*, previously believed to function as a sieve, showed most fluid moved tangential to the filtering combs rather than through them. The authors similarly suggested that tangential filtration may operate in concert with hydrosol filtration and sieving (Gerritsen et al. 1988). Given the great morphological diversity of aquatic filter- and suspension-feeders, the flows of many biological filters may be more hybrid-type in nature and the process of particle capture more complex than simply sieving.

Acknowledgements The investigation was supported in part by Grants from the US-Israel Binational Science Foundation (Grant #2012089 to K.R.S. and G.Y.), the Alfred P. Sloan Foundation (K.R.S.), Israel Science Foundation 1280/13 to G.Y., a Prof. Rahamimoff Travel Grant for Young Scientists (to K.R.C.), an Oregon Sea Grant 2014 Robert E. Malouf Marine Studies Scholarship (to K.R.C.), and a Julie and Rocky Dixon Graduate Innovation Award (to K.R.C.). We thank Raz Moskovich for flow cytometry assistance, and Peter Beninger, Evan Ward, Misty Paig-Tran, Hans Ulrik Riisgard, and Poul S. Larsen for useful comments and discussions.

Compliance with ethical standards

Ethical approval Ethical approval was not required for this research because ascidians are non-vertebrate chordates and as such are exempt from regulation by the Institutional Animal Care and Use Committee.

Conflict of interest The authors declare no conflicts of interests.

References

Acuña JL, Deibel D, Morris CC (1996) Particle capture mechanism of the pelagic tunicate *Oikopleura vanhoeffeni*. Limnol Oceanogr 41:1800–1814. https://doi.org/10.4319/lo.1996.41.8.1800

Alexander RM (1981) The chordates, 2nd edn. Cambridge University Press, Cambridge

Ali HA, Tamilselvi M (2016) Ecology of ascidians. Ascidians in coastal water. Springer International Publishing, Switzerland, pp 19–26. https://doi.org/10.1007/978-3-319-29118-5

Armsworthy SL, MacDonald BA, Ward JE (2001) Feeding activity, absorption efficiency and suspension feeding processes in the ascidian, *Halocynthia pyriformis* (Stolidobranchia: Ascidiacea): responses to variations in diet quantity and quality. J Exp Mar Biol Ecol 260:41–69. https://doi.org/10.1016/S0022-0981(01)00238-6

Beninger PG, Decottignies P, Guiheneuf F, Barillé L, Rincé Y (2007) Comparison of particle processing by two introduced suspension feeders: selection in *Crepidula fornicata* and *Crassostrea gigas*. Mar Ecol Prog Ser 334:165–177. https://doi.org/10.3354/meps334165

Bhave RR (1997) Cross flow filtration. In: Vogel HC, Todaro CL (eds) Fermentation and biochemical engineering hand-book. Noyes Publications, USA, pp 271–322

Bowen WR, Jenner F (1995) Theoretical descriptions of membrane filtration of colloids and fine particles: an assessment and review. Adv Colloid Interface Sci 56:141–200

Braimah SA (1987) Pattern of flow around filter-feeding structures of immature *Simulium bivittatum* Malloch (Diptera: Simuliidae) and *Isonychia campestris* McDunnough (Ephemeroptera: Oligoneuriidae). Can J Zool 65:514–521

Brainerd EL (2001) Caught in the crossflow. Nature 412:387–388

Champion JA, Katare YK, Mitragotri S (2007) Making polymeric micro- and nanoparticles of complex shapes. Proc Natl Acad Sci 104:11901–11904. https://doi.org/10.1073/pnas.0705326104

Chen CY (1955) Filtration of aerosols by fibrous media. Chem Rev 55:595–623. https://doi.org/10.1021/cr50003a004

Clavano WJ, Boss ES, Karp-Boss L (2007) Inherent optical properties of non-spherical marine-like particles—from theory to observation. Oceanogr Mar Biol Annu Rev 45:1–38

Cohen J (1988) Statistical power analysis for the behavioral sciences, 2nd edn. Academic Press, New York

Conley KR, Sutherland KR (2017) Particle shape impacts export and fate in the ocean through interactions with the globally abundant appendicularian *Oikopleura dioica*. PLoS One. https://doi.org/10.1371/journal.pone.0183105

Conley KR, Gemmell BJ, Bouquet J-M, Thompson EM, Sutherland KR (2017) A self-cleaning biological filter: how appendicularians mechanically control particle adhesion and removal. Limnol Oceanogr. https://doi.org/10.1002/lno.10680

Dadon-Pilosof A, Conley KR, Jacobi Y, Haber M, Lombard F, Sutherland KR, Steindler L, Tikochinski Y, Richter M, Glöckner FO, Suzuki MT, West NJ, Genin A, Yahel G (2017) Surface properties of SAR11 bacteria facilitate grazing avoidance. Nat Microbiol. https://doi.org/10.1038/s41564-017-0030-5

Deibel D, Lee SH (1992) Retention efficiency of sub-micrometer particles by the pharyngeal filter of the pelagic tunicate *Oikopleura vanhoeffeni*. Mar Ecol Prog Ser 81:25–30

Drost MR, Osse JWM, Muller M (1987) Prey capture by fish larvae, water flow patterns and the effect of escape movements of prey. Netherlands J Zool 38:23–45

Du Clos K (2016) Roles of siphon flows in suspension feeding. University of Maine, Orono

Dusenbery DB (1998) Fitness landscapes for effects of shape on chemotaxis and other behaviors of bacteria. J Bacteriol 180:5978–5983

Erika V, Werner B (1954) Über den Mechanismus des Nahrungserwerbs der Tunicaten, speziell der Ascidien. Helgoländer Meeresun 5:57–92. https://doi.org/10.1007/BF01609109

Fernández D, López-Urrutia Á, Fernández A, Acuña JL, Harris R (2004) Retention efficiency of 0.2 to 6 µm particles by the appendicularians *Oikopleura dioica* and *Fritillaria borealis*. Mar Ecol Prog Ser 266:89–101. https://doi.org/10.3354/meps266089

Flood PR (1982) Transport speed of the mucous feeding filter in *Clavelina lepadiformis* (Aplousobranchiata, Tunicata). Acta Zool 63:17–23. https://doi.org/10.1111/j.1463-6395.1982.tb00754.x

Flood PR, Fiala-Medioni A (1981) Ultrastructure and histochemistry of the food trapping mucous film in benthic filter-feeders (Ascidians). Acta Zool 62:53–65. https://doi.org/10.1111/j.1463-6395.1981.tb00616.x

Gerritsen J, Porter KG (1982) The role of surface chemistry in filter feeding by zooplankton. Science 216:1225–1227. https://doi.org/10.1126/science.216.4551.1225

Gerritsen J, Porter KG, Strickler JR (1988) Not by sieving alone: observations of suspension feeding in Daphnia. Bull Mar Sci 43:366–376

Goodbody I (1975) The physiology of ascidians. Adv Mar Biol 12:1–149. https://doi.org/10.1016/S0065-2881(08)60457-5

Guasto JS, Rusconi R, Stocker R (2012) Fluid mechanics of planktonic microorganisms. Annu Rev Fluid Mech 44:373–400. https://doi.org/10.1146/annurev-fluid-120710-101156

Herdman SWA (1899) Ascidia. Liverpool Marine Biology Committee, Liverpool

Ho CC, Keller A, Odell JA, Ottewill RH (1993) Preparation of monodisperse ellipsoidal polystyrene particles. Colloid Polym Sci 271:469–479. https://doi.org/10.1007/BF00657391

Holley MC (1986) Cell shape, spatial patterns of cilia, and mucus-net construction in the ascidian endostyle. Tissue Cell 18:667–684. https://doi.org/10.1016/0040-8166(86)90069-8

Jacobi Y, Yahel G, Shenkar N (2017) Efficient filtration of micron and submicron particles by ascidians from oligotrophic waters. Limnol Oceanogr. https://doi.org/10.1002/lno.10736

Jørgensen CB (1949) Feeding-rates of sponges, lamellibranchs and ascidians. Nature 163:912. https://doi.org/10.1038/163912a0

Jørgensen CB (1966) Biology of suspension feeding. Pergamon Press, New York

Jørgensen CB (1983) Fluid mechanical aspects of suspension feeding. Mar Ecol Prog Ser 11:89–103. https://doi.org/10.3354/meps011089

Jørgensen CB, Kørboe T, Møhlenberg F, Riisgård H (1984) Ciliary and mucus-net filter feeding, with special reference to fluid mechanical characteristics. Mar Ecol Prog Ser 15:283–292. https://doi.org/10.3354/meps015283

Kiørboe T (2011) How zooplankton feed: mechanisms, traits and trade-offs. Biol Rev 86:311–339

Knott NA, Davis AR, Buttemer WA (2004) Passive flow through an unstalked intertidal ascidian: orientation and morphology enhance suspension feeding in *Pyura stolonifera*. Biol Bull 207:217–224. https://doi.org/10.2307/1543210

Kustin K, Ladd KV, McLeod GC, Toppen DL (1974) Water transport rates of the tunicate *Ciona intestinalis*. Biol Bull 147:608–617

Labarbera M (1984) Feeding currents and particle capture mechanisms in suspension feeding animals. Integr Comp Biol 24:71–84. https://doi.org/10.1093/icb/24.1.71

Li X, Li J (2015) Dead-end filtration. In: Drioli E, Giorno L (eds) Encyclopedia of membranes. Springer, Berlin, pp 1–3

Loudon C, Alstad DN (1990) Theoretical mechanics of particle capture: predictions for hydropsychidae caddisfly distributional ecology. Am Nat 135:360–381. https://doi.org/10.1086/285051

MacGinitie GE (1939) The method of feeding of tunicates. Biol Bull 77:443–447

Mackie GO, Paul DH, Singla CM, Sleigh MA, Williams DE (1974) Branchial innervation and ciliary control in the ascidian Corella. Proc R Soc Lond B Biol Sci 187:1–35. https://doi.org/10.1098/rspb.1974.0058

Meijering E, Dzyubachyk O, Smal I (2012) Methods for cell and particle tracking. Methods Enzymol 504:183–200. https://doi.org/10.1016/B978-0-12-391857-4.00009-4

Millar RH (1971) The biology of ascidians. Adv Mar Biol 9:1–100. https://doi.org/10.1016/S0065-2881(08)60341-7

Morris CC, Deibel D (1993) Flow rate and particle concentration within the house of the pelagic tunicate *Oikopleura vanhoeffeni*. Mar Biol 115:445–452. https://doi.org/10.1007/BF00349843

Mota M, Teixeira JA, Yelshin A (2002) Influence of cell-shape on the cake resistance in dead-end and cross-flow filtrations. Sep Purif Technol 27:137–144. https://doi.org/10.1016/S1383-5866(01)00202-7

Orton JH (1913) The ciliary mechanisms on the gill and the mode of feeding in Amphioxus, ascidians, and *Solenomya tagata*. J Mar Biol Assoc UK 10:19–49

Paig-Tran EWM, Kleinteich T, Summers AP (2013) The filter pads and filtration mechanisms of the devil rays: variation at macro and microscopic scales. J Morphol 274:1026–1043. https://doi.org/10.1002/jmor.20160

Pennachetti CA (1984) Functional morphology of the branchial basket of ascidia paratropa (Tunicata, Ascidiacea). Zoomorphology 104:216–222. https://doi.org/10.1007/BF00312033

Petersen JK (2007) Ascidian suspension feeding. J Exp Mar Biol Ecol 342:127–137

R Core Team (2013) R: A language and environment for statistical computing. R Foundation for Statistical Computing, Vienna, Austria. http://www.R-project.org/

Riisgård HUH (1988) The ascidian pump: properties and energy cost. Mar Ecol Prog Ser 47:129–134. https://doi.org/10.3354/meps047129

Riisgard HU, Larsen PS (2001) Minireview: ciliary filter feeding and bio-fluid mechanics- present understanding and unsolved problems. Limnitiol Ocean 46:882–891. https://doi.org/10.4319/lo.2001.46.4.0882

Riisgård HU, Larsen PS (2000) A comment on experimental techniques for studying particle capture in filter-feeding bivalves. Limnol Oceanogr 45:1192–1195

Riisgård HU, Larsen PS (2005) Water flow analysis and particle capture in ciliary suspension-feeding scallops (Pectinidae). Mar Ecol Prog Ser 303:177–193. https://doi.org/10.3354/meps303177

Riisgård HU, Larsen PS (2010) Particle capture mechanisms in suspension-feeding invertebrates. Mar Ecol Prog Ser 418:255–293

Rubenstein DI, Koehl MAR (1977) The mechanisms of filter feeding: some theoretical considerations. Am Nat 111:981–994. https://doi.org/10.2307/2460393

Sanderson SL, Cheer AY, Goodrich JS, Graziano JD, Callan WT (2001) Crossflow filtration in suspension-feeding fishes. Nature 412:439–441. https://doi.org/10.1038/35086574

Schneider CA, Rasband WS, Eliceiri KW (2012) NIH Image to ImageJ: 25 years of image analysis. Nat Methods 9:671–675. https://doi.org/10.1038/nmeth.2089

Schwartz L, Seeley KL (2002) Introduction to tangential flow filtration for laboratory and process development applications. Pall Life Sciences, Ann Arbor, pp 1–12. https://laboratory.pall.com/content/dam/pall/laboratory/literature-library/non-gated/id-34212.pdf

Shimeta J (1993) Diffusional encounter of submicrometer particles and small cells by suspension feeders. Limnol Oceanogr 38:456–465. https://doi.org/10.4319/lo.1993.38.2.0456

Shimeta J, Jumars P (1991) Physical mechanisms and rates of particle capture by suspension feeders. Oceanogr Mar Biol Annu Rev 29:191–257. https://doi.org/10.1016/j.jembe.2004.08.013

Silverman H, Lynn JW, Beninger PG, Dietz TH (1999) The role of latero-frontal cirri in particle capture by the gills of *Mytilus edulis*. Biol Bull 197:368–376

Silvester NR (1983) Some hydrodynamic aspects of fitter feeding with rectangular-mesh nets. J Theor Biol 103:265–286. https://doi.org/10.1016/0022-5193(83)90028-0

Smith JC, Sanderson SL (2007) Mucus function and crossflow filtration in a fish with gill rakers removed versus intact. J Exp Biol 210:2706–2713

Song L, Elimelech M (1995) Theory of concentration polarization in crossflow filtration. J Chem Soc Faraday Trans 91:3389. https://doi.org/10.1039/ft9959103389

Spielman L, Goren SL (1968) Model for predicting pressure drop and filtration efficiency in fibrous media. Environ Sci Technol 2:279–287. https://doi.org/10.1021/es60016a003

Sutherland KR (2010) Form, function and flow in the plankton: jet propulsion and filtration by pelagic tunicates. PhD dissertation, Massachusetts Institute of Technology and Woods Hole Oceanographic Institution, Woods Hole

Sutherland KR, Madin LP, Stocker R (2010) Filtration of submicrometer particles by pelagic tunicates. Proc Natl Acad Sci 107:15129–15134. https://doi.org/10.1073/pnas.1003599107

Turon X (1990) Estructura de los filtros branquiales de ascidias (tunicados). Misc Zool 14:125–133

Visser AW, Jonsson PR (2000) On the reorientation of non-spherical prey particles in a feeding current. J Plankton Res 22:761–777. https://doi.org/10.1093/plankt/22.4.761

Vogel S (1994) Life in moving fluids: the physical biology of flow. Princeton University Press, Princeton

Ward JE, Sanford LP, Newell RIE, MacDonald BA (1998) A new explanation of particle capture in suspension-feeding bivalve molluscs. Limnol Oceanogr 43:741–752. https://doi.org/10.4319/lo.1998.43.5.0741

Ward JE, Sanford LP, Newell RIE, MacDonald BA (2000) The utility of in vivo observations for describing particle capture processes in suspension-feeding bivalve molluscs. Limnol Oceanogr 45:1203–1210

Wotton RS (1994) Methods for capturing particles in benthic animals. The biology of particles in aquatic systems. Lewis Publisher, Boca Raton, pp 183–204

Wright SH, Stephens GC (1978) Removal of amino acid during a single passage of water across the gill of marine mussels. J Exp Zool 205:337–351. https://doi.org/10.1002/jez.1402050302

Young CM, Braithwaite L (1980) Orientation and current-induced flow in the stalked ascidian *Styela montereyensis*. Biol Bull 159:428–440